Anuário do Instituto de Geociências - UFRJ
www.anuario.igeo.ufrj.br

Sea Surface Temperature Optimization Evaluation in the Passage of an Explosive Cyclone in the Southwest Atlantic Ocean

Avaliação da Otimização da Temperatura da Superfície do Mar durante a Passagem de um Ciclone Explosivo no Sudoeste do Oceano Atlântico

Ana Cristina Pinto de Almeida Palmeira[1]; Ricardo de Camargo[2] & Ronaldo Maia de Jesus Palmeira[2]

1Universidade Federal do Rio de Janeiro, Instituto de Geociências, Departamento de Meteorologia.
Av. Athos da Silveira Ramos 274. Cidade Universitária, 21941-916, Rio de Janeiro, RJ, Brasil
2Universidade de São Paulo, Instituto de Astronomia, Geofísica e Ciências Atmosféricas,
Departamento de Ciências Atmosféricas. Rua do Matão 1226. Cidade Universitária, 05508-090. São Paulo, SP. Brasil
E-mails: anactn@gmail.com; ricamarg@usp.br; palmeira@gmail.com
Recebido em: 10/01/2019 Aprovado em: 04/04/2019
DOI: http://dx.doi.org/10.11137/2019_2_245_258

Resumo

Na modelagem numérica do tempo, a atualização da Temperatura da Superfície do Mar (TSM) pode influenciar fenômenos atmosféricos em diferentes escalas. Sendo assim, um modelo simplificado da Camada de Mistura Oceânica (CMO) foi incluído como uma sub-rotina no Brazilian Regional Atmospheric Modeling System (BRAMS) de forma a atualizar a temperatura da superfície do mar (TSM) a cada passo de tempo, com baixo custo computacional. Comparações foram realizadas entre simulações atmosféricas usando uma CMO dinâmica e a TSM climatológica, padrão do BRAMS. Houve variações diretas significativas nos fluxos de calor latente e sensível, bem como na nebulosidade, de modo que quanto mais aquecida a TSM, maior a resposta dessas variáveis. Por outro lado, embora não tenha havido aumento significativo nas taxas de precipitação, houve maior precipitação quando a TSM foi maior. As variações na pressão ao nível do mar foram da ordem de 1-2 hPa, indicando que as variações nos fluxos de superfície estão relacionadas à manutenção e persistência dos sistemas e não ao seu aprofundamento.
Palavras-chave: fluxos de calor; camada de mistura oceânica; ciclone extratropical

Abstract

In numerical weather prediction, the updating of the Sea Surface Temperature (SST) can influence atmospheric phenomena on different scales. Thus, a simplified model of the oceanic mixed layer (OML), was included as a subroutine in the Brazilian Regional Atmospheric System (BRAMS) in order to update the SST at each time step, with low computational cost. Comparisons between atmospheric simulations using an active OML and climatological SST mask, which is part of the BRAMS model, were made. There were significant direct variations in the latent and sensible heat fluxes as well as in cloudiness: the warmer the SST, the greater the response of these variables. On the other hand, although there was no significant increase in precipitation rates, there was higher rainfall when the SST was higher. The variations in the sea level pressure were to the order of 1-2 hPa, indicating that the variations in surface flows are related to the maintenance and persistence of systems and not to their deepening.
Keywords: heat fluxes; oceanic mixed layer; extratropical cyclone

1 Introduction

The region of the southwest Atlantic is marked by the predominance of the South Atlantic Subtropical Anticyclone (SASA) and the passage of both transient and stationary systems, such as cyclones. Necco (1982) studied cyclonic vortices with parallel displacements to shorelines related to ocean currents and found that the cyclonic vortex at 500 hPa is necessary, but not enough, to develop convection; he also observed that the sensible heat is more important for the intensification of tropical cyclones.

Gan & Rao (1991) found two well-marked surface cyclogenesis clusters at South America: one in the Gulf of San Matias and the another over Uruguay. These two centres exist all year round. The Uruguayan one is more intense in the winter and the Gulf of San Matias centre is more intense in the summer. In the transition seasons the quantity is little different.After this, Reboita (2008) confirmed the same regions and found one closer to the south and south-eastern coast of Brazil.

Seluchi (1995) evaluated 54 cases of cyclogenesis in the South American continent and discovered that the events can be detected up to five days in advance by monitoring troughs with long waves that can move to above 35°S, in the range of greater baroclinicity. He concluded that coastal cyclogenetic processes usually take place during the winter and spring and gradually decrease their frequency during the summer and early fall.

Sugahara (2000), analysing the low-pressure systems and tropical cyclones in South America from 1985 to 1993, found little variation in the frequency of cyclones, though he did find a subtle increase in the winter months.

Based on data from the National Centers for Environmental Prediction (NCEP) Reanalysis for the period 1980 to 1999, Palmeira (2003) conducted a climatological analysis of cyclones over the South Atlantic, and found that in all seasons the highest frequencies occur at latitudes above 50°S, and there were more than 200 occurrences at above 60°S. At lower latitudes, the frequency of cyclogenesis decreases, but it is interesting to note that the increased occurrence of cyclogenesis at lower latitudes triples in winter compared to the summer period (latitude 32.5°S).

According to Bosart & Lackmann (1995), depending on the stage of development of atmospheric cyclone, the flow of latent and sensible heat, essential for the initial phase, may even weaken the cyclone, reducing the baroclinicity at low levels, and reducing thermal advection and consequently the rate of deepening. Warming by latent heat release dominates the baroclinic processes in explosive maritime cases.

Sinclair (1995), evaluating cyclones over the South Atlantic, found a slight increase in the release of latent heat on SST at low latitudes, causing higher drops in pressure, whereas Saraiva (1996) found through numerical modelling in the passage of an explosive cyclone in the Southwest Atlantic that the release of latent and sensible heat of the Brazil-Malvinas Confluence was the key to its rapid intensification, modulating its trajectory and the microphysics of low clouds.

Silva *et al.* (2004) presented simulations of cyclone Catarina using BRAMS model (Freitas *et al.*, 2017) to identify the impact of the SST conditions in the Atlantic Ocean region, imposing positive and negative anomalies on the SST field (+ / - 2°C). In the case of the experiment with warmer SSTs there was an increase in the cumulative rainfall, while cooler SSTs resulted in a decrease in rainfall (13% and 35%, respectively). It is noteworthy that the trajectory of the cyclone did not change due to the large-scale dynamics.

Pezzi *et al.* (2005) found that the Marine Atmospheric Boundary Layer (MABL) is modulated by the strong SST gradient, and an explanation for this is since the MABL self-adjusts to changes in the SST. Positive SST anomalies induce changes in the static stability of the MABL. In this case, the buoyancy and turbulence increase over warm waters and decrease the vertical wind shear in the MABL, generating stronger surface winds. The opposite would be expected over cooler waters.

To contribute to the understanding of the ocean-atmosphere processes that occur in the Southwest Atlantic, this study aims to determine the importance of the correction of the SST for the specification of meteorological models in terms of the impact on the development and evolution of transient weather systems under different synoptic patterns. For this purpose, a simplified model of mixed layer ocean, included in a BRAMS subroutine model, was used to assess changes in the air-sea interface and investigate the physical mechanisms involved in the atmospheric column. This is an original study in numerical atmospheric mesoscale modelling and the importance of short-term temporal variations. The inclusion of the SST variation in the correction of the surface energy balance will allow the behaviour of the interface processes to be better understood and will provide more information on the issue of thermodynamic coupling between atmospheric and ocean models.

The SST also varies according to local situations; for example, in the presence of a cyclone, radiative effects are negligible near the centre due to the presence of a thick layer of clouds which, in addition to reflecting almost all the incidental short-wave radiation, block the loss of long-wave radiation. Friehe *et al.* (1991) investigated the effect of SST fronts on the structure of the Atmospheric Boundary Layer (ABL) during the FASINEX (Front Air-Sea INteraction EXperiment) and demonstrated that the hot air flowing over cold water leads to a stable and shallow ABL, while cold air flowing over warm water leads to an unstable and increasing ABL.

Like the atmosphere, the ocean also has an internal boundary layer next to surface. This region is called the Oceanic Mixed Layer (OML) and is fully turbulent due to its mix, and its thermodynamic properties (T, ρ) are considered approximately vertically constant. The mix is direct through the wind and indirect by the waves.

According to Chu (1993), in high winds, the OML deepens due to increased turbulent kinetic energy (TKE) generated by the wind being strong enough to push the cold water at the base of the OML. Excessive heat loss at the base (entrainment heat flux) over the net heat gain at the surface leads to the cooling of the OML. The thinner (thicker) the OML, the cooler (warmer) it is, leaving the ΔSST/Δt and the depth positively correlated. With light winds, the TKE in the OML generated by the wind is insufficient to push the stable deep water (cold and stratified), and as the net heat gain at the ocean surface is much smaller than the heat loss at the base of the OML, it becomes warmer. The narrower (wider) the OML, the more it warms (cools), leaving ΔSST/Δt and the depth of the OML is negatively related.

Thus, the fundamental physical aspects of both the ocean and the atmosphere are presented in Section 1, with the objective. The description of the aspects of interest relating to the numerical part and the choice of the specific case investigated by means of numerical experiments are presented in Section 2. Section 3 gives the simulations and results. Section 4 will treat the discussion while Section 5 summarizes the conclusions.

2 Materials and Methods

In order to make numerical simulations of the cyclone, the BRAMS (Freitas *et al.*, 2017) atmospheric model was used, with initial and contour conditions of the NCEP Reanalysis database (Kalnay *et al.*, 1996).

The NCEP database also contributed to a preliminary analysis of the synoptic atmosphere scenario that led to the cyclone's life cycle.

To verify the thickness of the OML, we used simulations of the HYbrid Coordinate Ocean Model (HYCOM, Bleck *et al.*, 2002) ocean circulation model, available in the Brazilian Navy, in addition to the LEVITUS (Levitus & Boyer, 1994) data base.

2.1 The BRAMS Atmospheric Model

For the atmospheric part of the study, the BRAMS, which is a limited area model, was chosen. The version used in this study was the 5.4 plus (Fazenda *et al.*, 2006), which has sets of shallow cumulus parameterization for shallow and deep convection, including a mass flux scheme with several closures, based on Grell & Devenyi (2002). The initial function of the convective parameterization uses Turbulent Kinetic Energy (TKE) of the Planetary

Boundary Layer (PBL) to modulate the maximum distance at which the plots may deviate from their source and uses this distance to determine whether a given grid column will maintain convection or not. The vegetation data with 1 km resolution are derived from the International Geosphere-Biosphere Programme 2.0 (IGBP, 1986) data sets, and the daily initialization of soil moisture may also be used (Gevaerd & Freitas, 2006). The details of the observed parameters of the South American biomass may be used for a more realistic specification of surface features. There was a normalization of the data set of the vegetation index (NDVI), which is derived from the MODIS (Moderate Resolution Imaging Spectroradiometer - Carroll *et al.* (2003)) data set, based on the years 2001-2002, processed by the Terrestrial Biophysics and Remote Sensing Lab and converted into the BRAMS format and structure. Thus, several biophysical parameters associated with the soil parameterizations and the BRAMS vegetation were adapted to tropical and subtropical biomes and soils, using observations or estimates obtained from field campaigns associated with the LBA (Large Scale Biosphere-Atmosphere Experiment in Amazonia - Silva Dias *et al*. (2002)).

Its computational capabilities include the assimilation of heterogeneous soil moisture, cyclic operating assimilation, SIB2.5 (Simplified Simple Biosphere Model) surface parameterization, besides the serial and parallel options. The following section gives a summary of the configuration of the model (Table 1).

2.2 Including the OML Module to Differentiate the BRAMS SST

To provide a new option to treat the SST during the simulation, an OML module was included to predict the SST at every time step and not simply to assimilate the information available on a climatological, weekly or daily basis. Therefore, the classic model of Kraus & Turner (1967) [here in after K-T] was chosen in order to make a routine public (mxkrtm.f) ocean circulation HYCOM, and then direct the study to the branch of research that uses synchronous simulations to investigate ocean-atmosphere coupling. To verify the result of the variation of the height and temperature of the OML (hence the SST) to consider both thermodynamic factors and ocean dynamics we used the HYCOM ocean model itself, in the K-T model, the same methodology routinely used in this study. The HYCOM ocean circulation model provides different options for the OML. One of them is that of K-T.

In simulations with an active OML, data from the LEVITUS Climatology were used as a profile (initial estimate) to find the height of the base of the OML and the thermocline, necessary for the K-T model. After this verification, the value of the BRAMS climatological SST was compared with the LEVITUS data, and then a difference was made in the whole profile so that the SST in the case of the active OML was adjusted to the difference of the value of the climatological SST and this temperature difference was spread to the final depth of the OML (estimated by LEVITUS). Thereafter (from the thermocline), the BRAMS module took on the Levitus climatological profile without any changes. From the next moment, the active OML now presented a new profile, calculated by the K-T model.

2.3 Simulated Event: Explosive Cyclone

The case chosen was the explosive cyclone from 22 to 26 July 2007, which, after being formed, moved quickly to the Southeast, deepening (Figures 1 and 2) and changing its initial characteristics, according to the phase diagram (Hart, 2003).

Brams Configurations	
Integration time: 21 to 28 September	**Cumulus:** Grell & Devenyi (2002)
Horizontal resolution: 30 km	**Microphysics:** Level 3
Nudging source: Global data every 6 h	**Shallow Cumulus:** on
Center field: 27.5°S/045°W	**Radiation:** Chen & Cotton (1983)
Number of points at x: 146	**Round:** Serial
Number of points at y: 166	**Output frequency:** 1 hour
Sigma vertical levels: 28	**Initial OML:** Levitus Climatology
Vertical spacing: 50 m from the surface with an amplification factor of 1.2 to a height of 1 Km. Above this, the spacing becomes constant and equal to 1 km	**Horizontal diffusion coefficients:** Smagorinsky (1963) **Vertical diffusion coefficients:** Mellor & Yamada (1982)

Table 1 Summary of the configuration used in the BRAMS model.

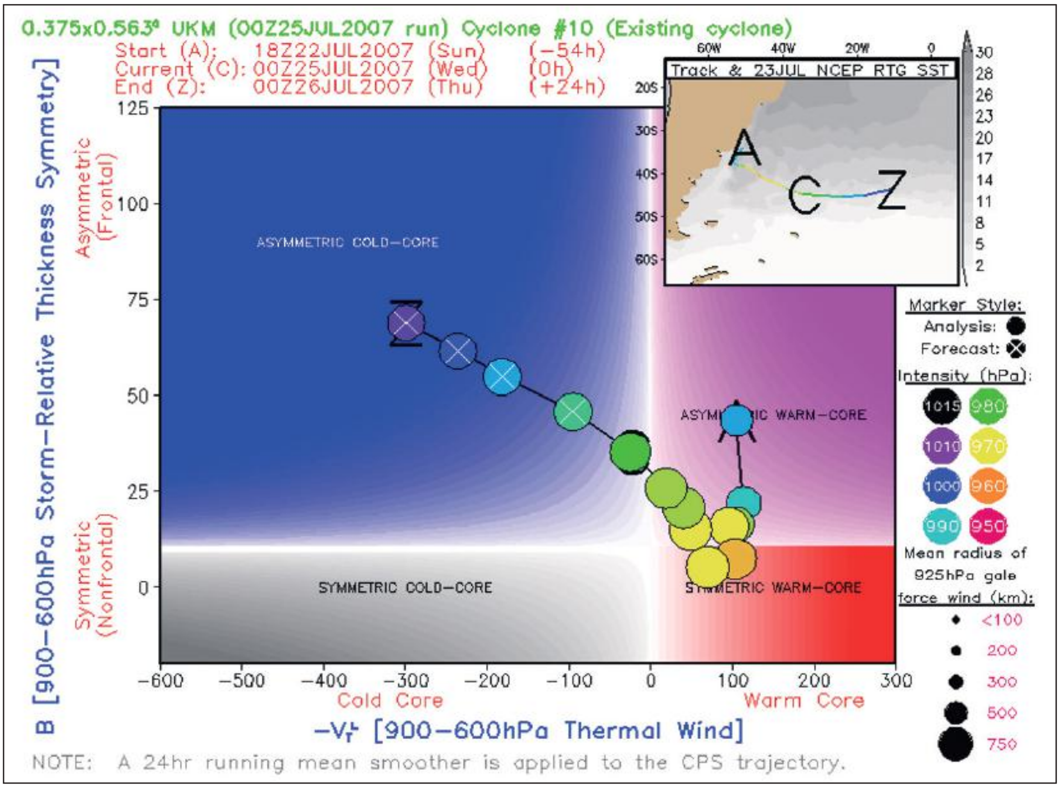

Figure 1 Phase diagram of the explosive cyclone in July 2007 (Shared and kindly provided by Robert Hart at http://moe.met.fsu.edu/cyclonephase).

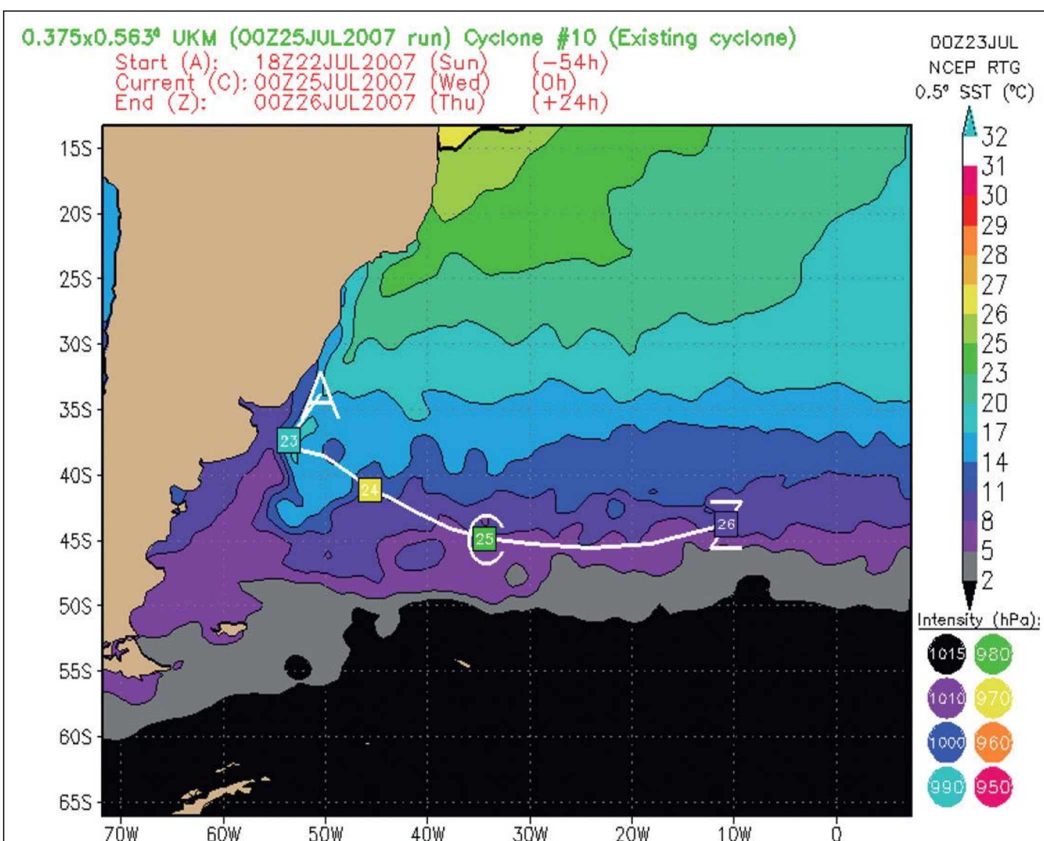

Figure 2 Track of the explosive cyclone in July 2007 (Shared and kindly provided by Robert Hart at http://moe.met.fsu.edu/cyclonephase).

Through the NCEP Reanalysis (Figures 3 and 4), atmospheric pattern fields are shown where it can be noted that the region suffered post-frontal influences with an extratropical cyclone in the extreme southwest leaving the domain, and another low region (1002 hPa) over the continent (26°S/058°W), which shifted to the southeast with the dynamic support at 200 hPa.

Both cyclones had soft core release of surface latent heat and upward motion of 850 hPa. On 23JUL2007-00Z the cyclone also deepened (996 hPa), this time with support at middle to high levels. The meridionally aligned upward movement presented a higher amount of latent heat release, confirming its deepening.

In the next six hours, the trough extended to the coast of the state of São Paulo, and the cyclone deepened (989 hPa) and gradually moved to the south (37°S/050°W), still supported at 200 hPa. The region of the cold front marked an upward movement and a core of latent heat release.

A cold front completely moved away eastward from the coastline on 24JUL2007-00Z, while the extratropical cyclone moved slowly south-eastward, deepening (972 hPa) at 42°S/045°W. It should be noted that the large region of latent heat release was associated to the post-frontal regime, where the cold air flowed over the relatively warmer SST.

The information on the OML provided by the HYCOM and about SST from MODIS/AQUA satellite (Advanced Microwave Scanning Radiometer sensor, AMSR-E) for this case (Figure 5 A and B) indicates an initially warm and not very deep pattern (18°C - 21°C) followed by a slight narrowing and cooling (15°C) in the region off the Santa Catarina, southern coast of Brazil. However, the SST pattern for this period (Figure 5) indicates a marked zonal gradient in the region of cyclone intensification typical of favouring the lowering of surface pressure (Saraiva, 1996).

3 Results

On average, it can be observed from Figure 6 (A and B) that the presence of the OML causes SST variations up to 3°C the main one in the dipole off the coast of the state of Rio Grande do Sul. The sensible heat indicated greater differences than the latent heat, both in intensity and in areas of the domain (Figure 7 and 8), which were related to the direct differences between the air temperature and the SST (figure not shown).

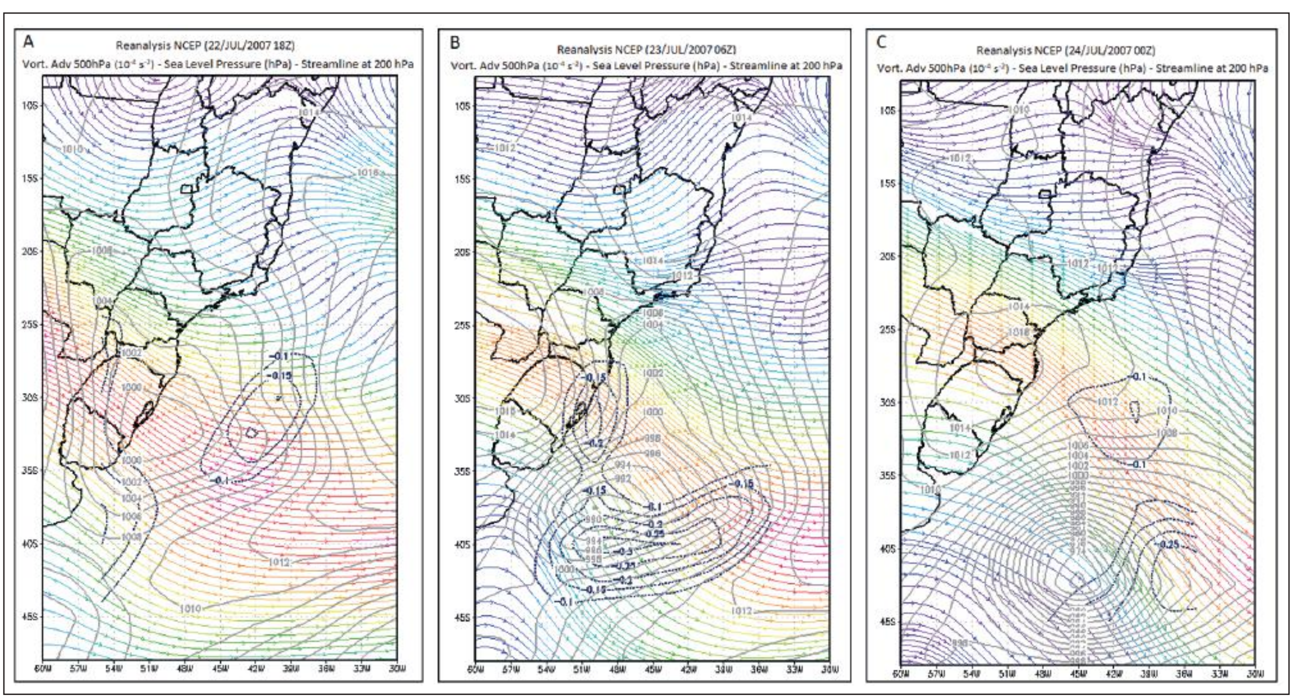

Figure 3 Mean sea level pressure in hPa (gray lines), advection of relative vorticity at 500 hPa in 10^{-4} s^{-2} (dotted dark blue) and streamlines at 200 hPa from the NCEP reanalysis from 22 July 2007 to 24 July 2007.

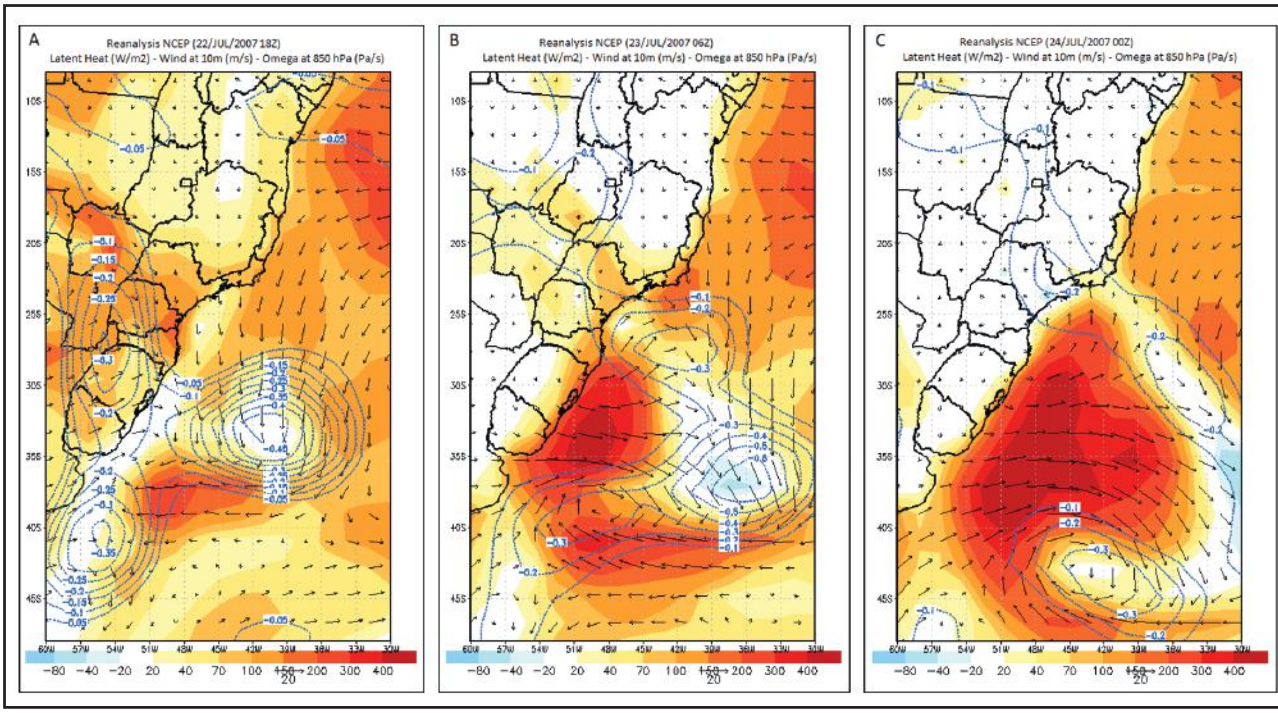

Figure 4 Latent heat flux in Wm^{-2} (shaded), wind at 10 meters in ms^{-1} (vectors) and 850 hPa omega in Pa.s^{-1} (dark blue contours), from the NCEP reanalysis of data from 22 July 2007 to 24 July 2007.

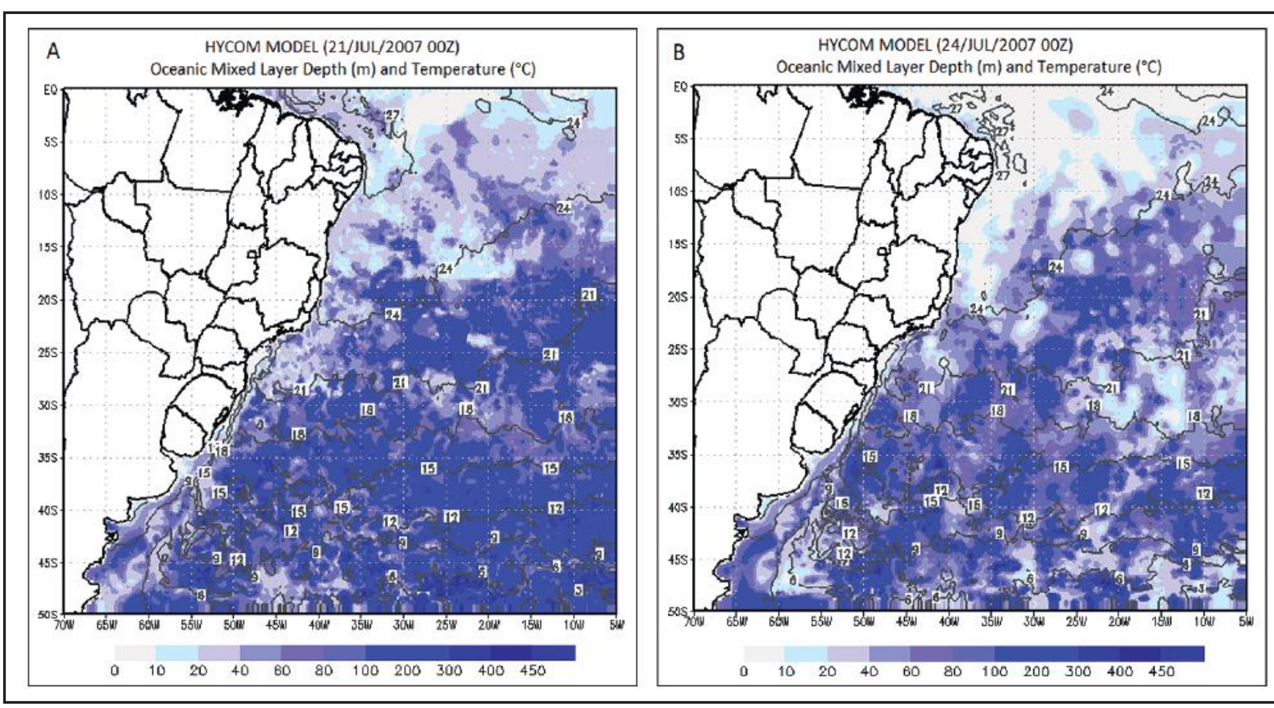

Figure 5: OML depth in meters from the HYCOM model for the July 2007 case and SST (°C) from satellite AQUA AMSR-E's at 0000 Z between 21 and 24 July 2007.

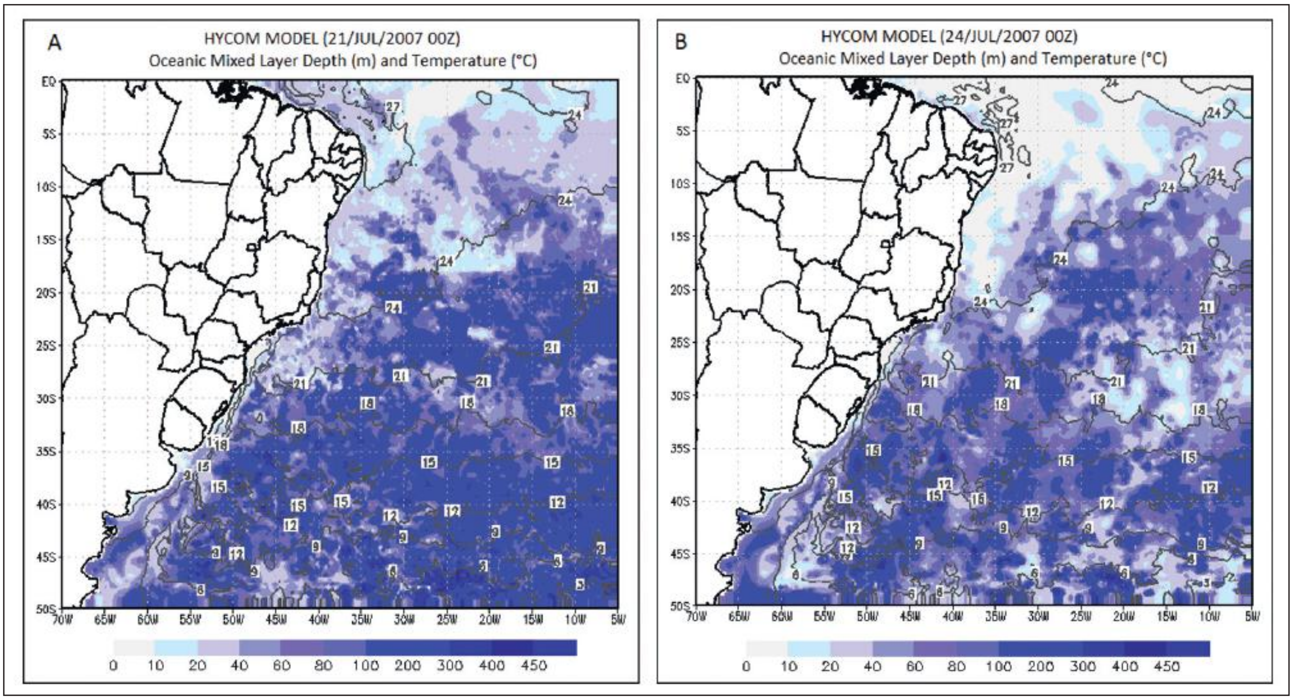

Figure 6 Differences between the fields of sea surface temperature in Celsius.

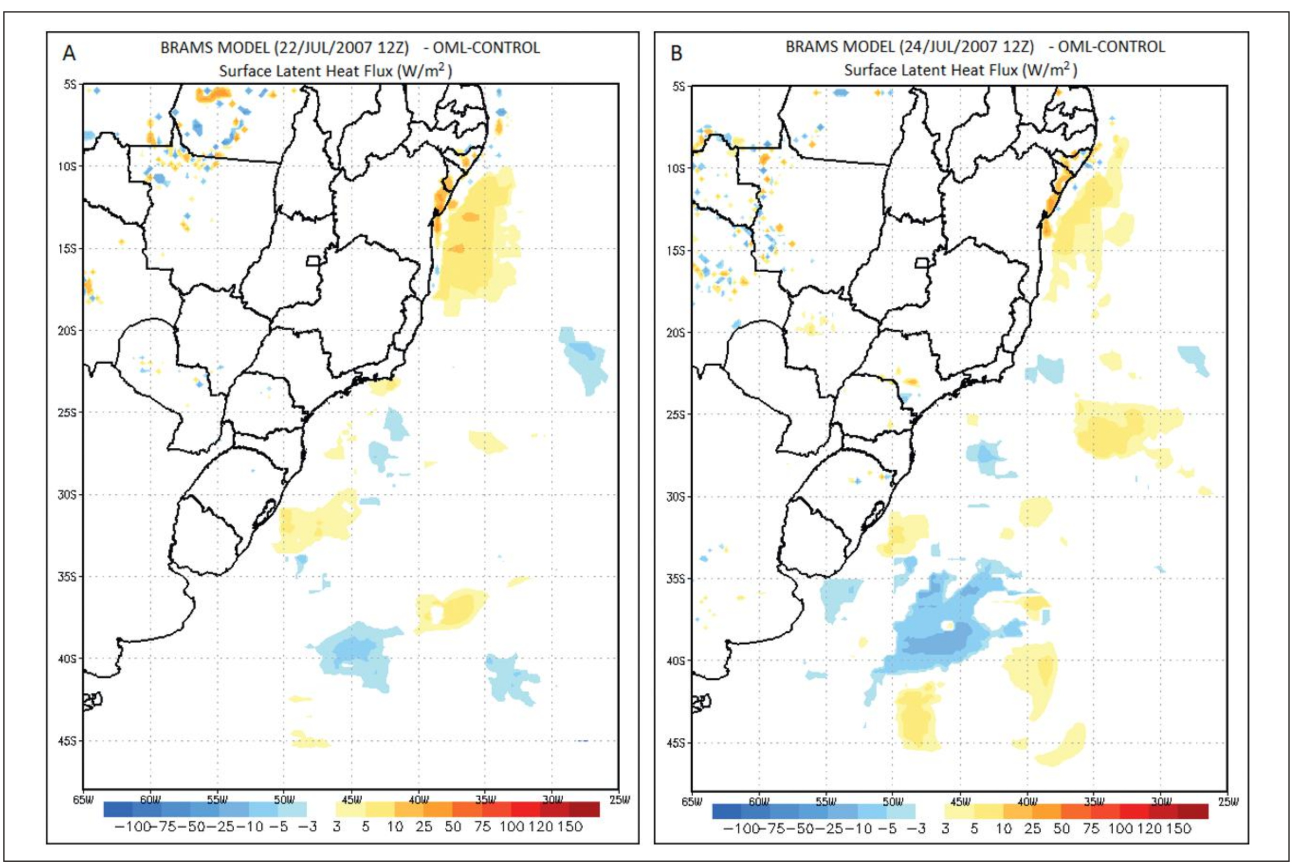

Figure 7 Differences between the fields of latent heat in Wm^{-2}.

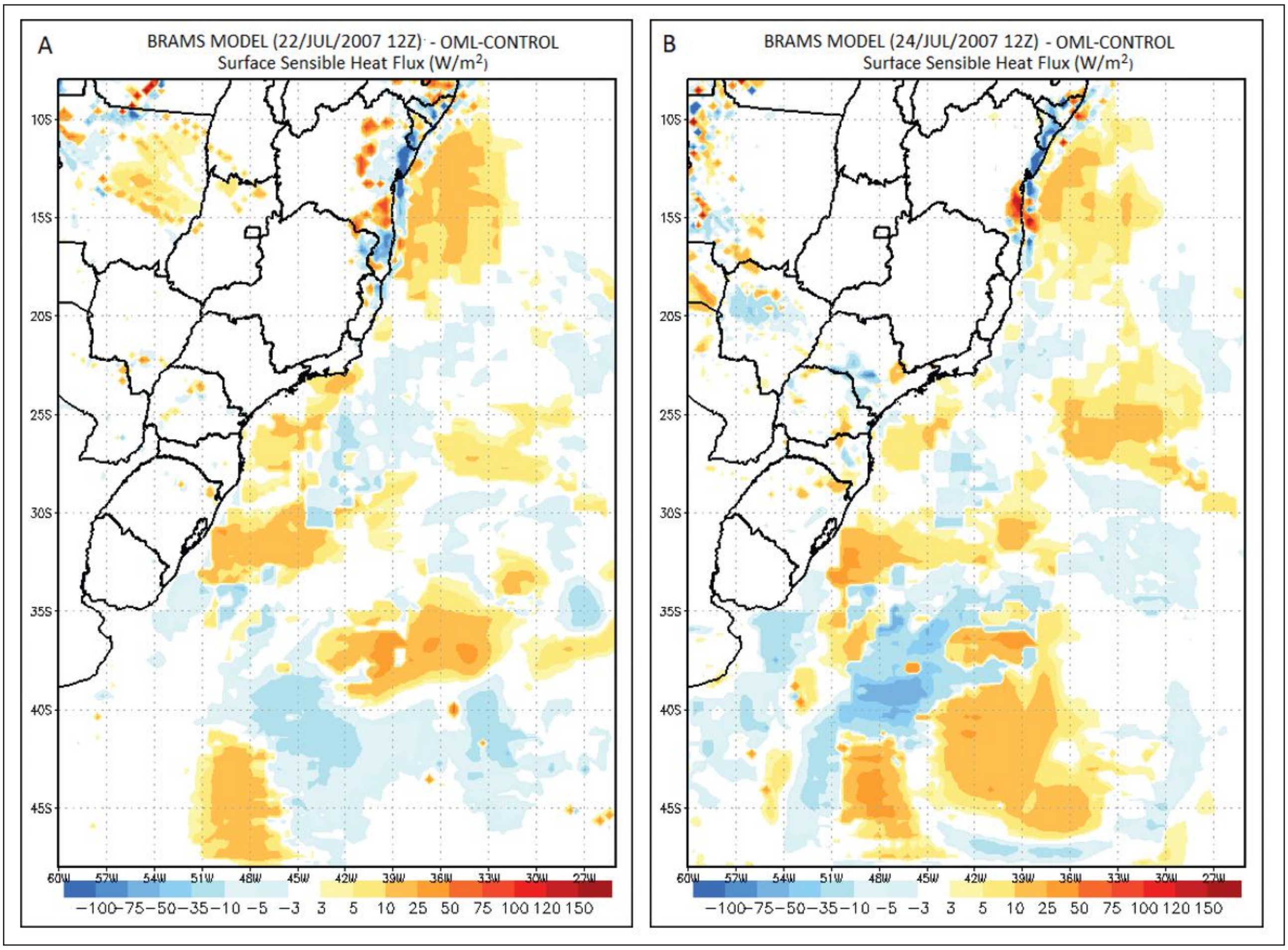

Figure 8 Differences between sensible heat flux fields in Wm^{-2}.

Two main points were chosen to investigate the most relevant time series. The first was at 34°S/50°W, where the cyclone was formed (Figure 9). The pressures and winds were synchronous, and there was very little difference in vertical movements. The variables in the control case showed slightly higher values than the active OML case. The SST difference was around 1°C, the precipitation 0.1 mm/h, the value of the maximum difference of latent heat reached 20 Wm^{-2}, and the sensible heat 30 Wm^{-2}. It is noteworthy that the SST control was higher than in the case of the active OML.

In terms of vertical profile (Figure 10), there was a large increase of moisture at all levels plus a cooling profile, an excellent feature for an increase of low pressure. By comparison, the control case also presents higher potential temperature (theta) values (between 1.0°C and 1.5°C), and lower mixing ratios (0.6 g/kg) most of the time, with the humidity difference reaching levels of 650 hPa.

Another point chosen was 40°S/50°W, where the cyclone deepened significantly. Figure 11 shows that the sea level pressure in the simulation with an active OML from 24 July is slightly larger than that of the control case, as is the case of the upward movement. As the SST is greater in the control case (about 2°C), this is reflected in the flow of latent and sensible heat and in most of the period in wind strength. It can also be seen that the change in wind direction occurs slightly before in the active OML case, with a slight time lag, and with the control case greater than the active OML case.

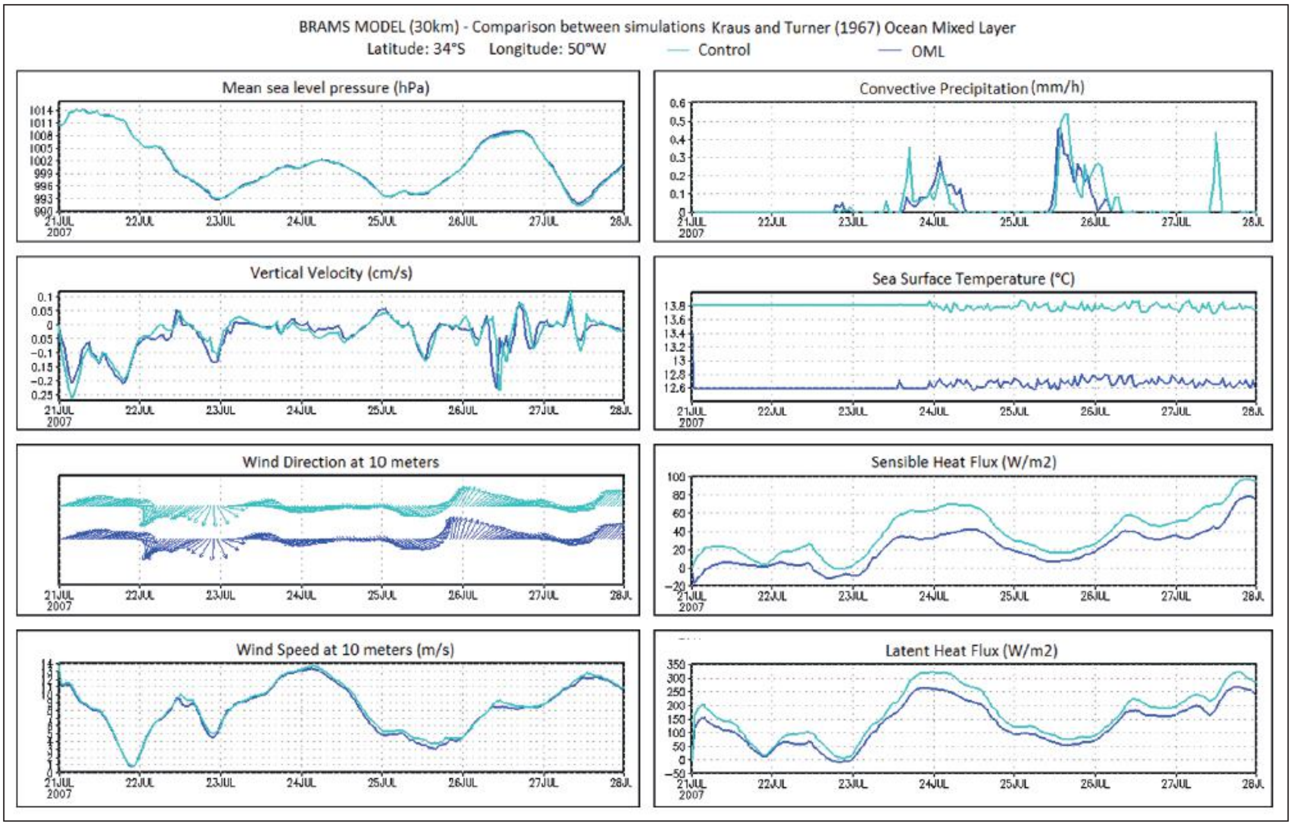

Figure 9 Time series of comparisons between the atmospheric variables in the models with climatological SST (control) and active OML at the point 34°S/050°W.

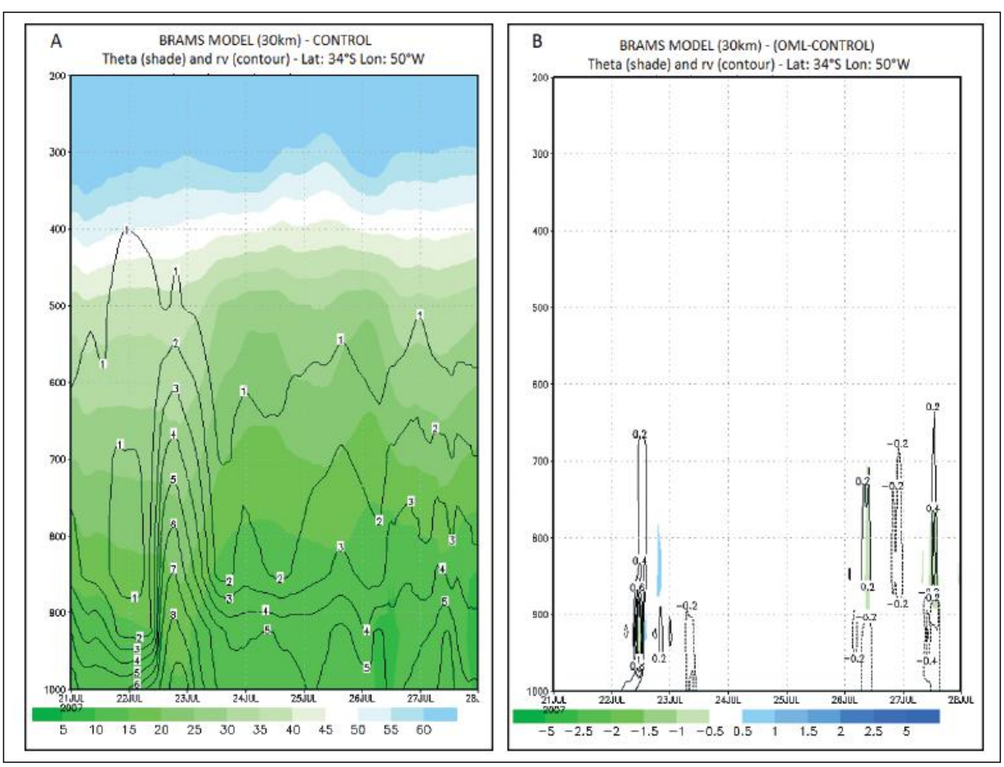

Figure 10: Time series profile of the theta (°C) and mixing ratio profile (g/kg) for the control case A and the difference between the ACTIVE OML and CONTROL cases B at the point 34°S/050°W.

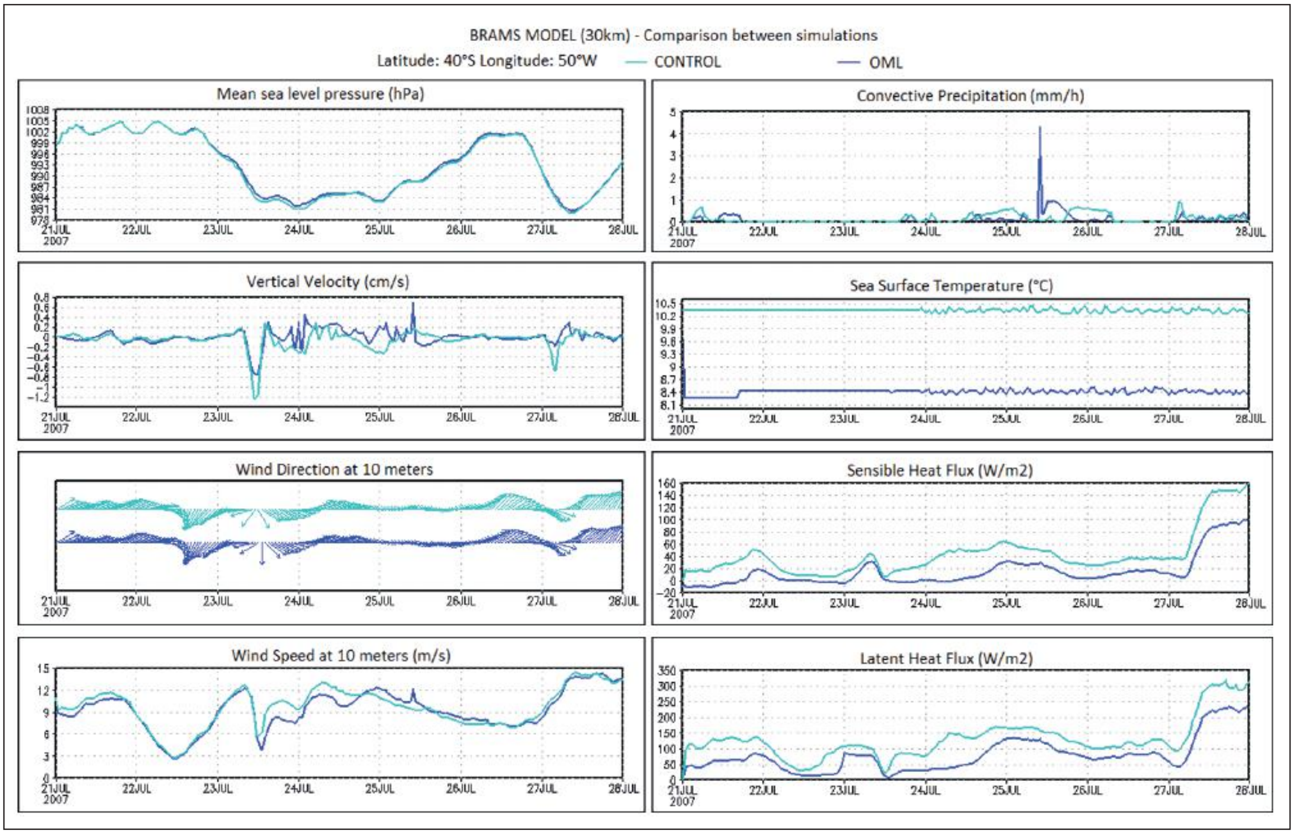

Figure 11 Time series of comparisons between the atmospheric variables in the models with climatological SST (control) and active OML at the point 40°S/050°W.

In terms of the vertical profile (Figure 12), it was generally noticed that there was plenty of moisture available at low and middle levels, with the middle levels slightly cooler and drier on 22 and 23 July, thus favouring convection. By comparison, the control case also presented higher potential temperature (theta) values (1.5°C) and mixing ratio (0.6 g/kg) for most of the period, reaching middle levels (400 hPa).

4 Discussion

The points selected were near cyclones (and not exactly under them), with the precaution of avoiding the cores of intense convective activity. Thus, in the rare moments of rain detected at each point, the control case SST was warmer than the active OML case. In these events, the precipitation of the active OML case behaved more persistently than in the control case, although the latter showed higher rates of precipitation. This result is consistent with previous studies in which the greater rainfall is directly related to higher surface temperatures (Silva *et al*., 2004). It is worth noting that although the rain did not significantly differ (to the order of 1 mm/h), the formation of clouds was well marked at times, being greater when the SST showed higher values.

The difference field of SST (OML-CONTROL) produced large variations in the initial moments, maintaining differences of about 1 to 5°C, regardless of the atmospheric phenomenon studied, since the adjustment of the profile characteristics of the OML of the LEVITUS climatological base diverged from the BRAMS climatological SST at most points, as evidenced in the Brazil-Malvinas confluence region. However, once the SST was adjusted, there was little change over time (about 1°C). It was also interesting to note that despite these subtle differences in SSTs, heat fluxes were expressed in an effective and direct way: the higher (lower) the SST, the larger (smaller) the fluxes of latent and sensible heat.

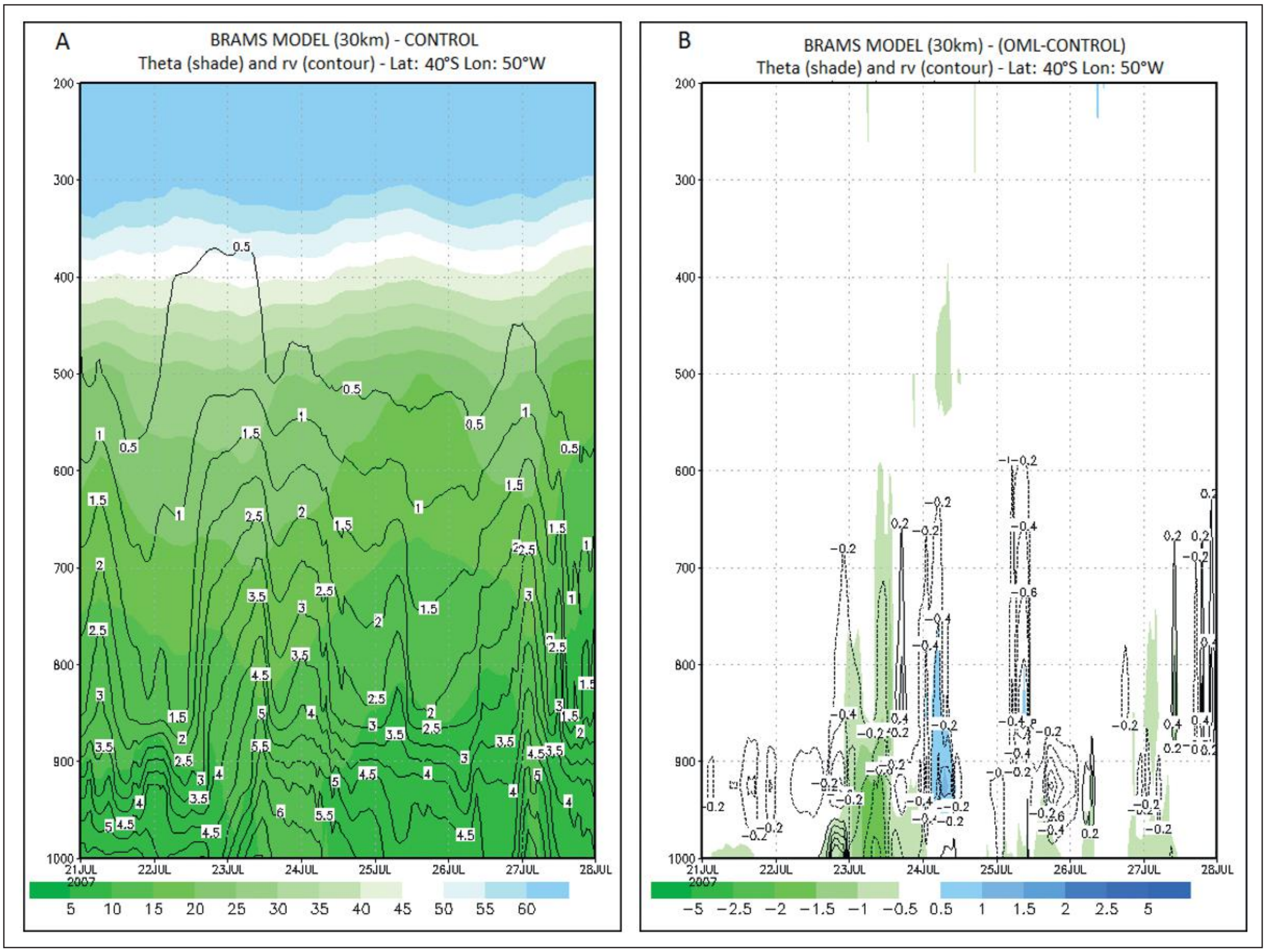

Figure 12 Time series of the theta (°C) and mixing ratio profile (g/kg) for the control case A and the difference between the ACTIVE OML and CONTROL cases B at the point 40°S/050°W.

The sensible heat field showed higher discrepancies between simulations when compared to the differences between latent heat. As the amount of sensible heat is a direct measurement between the air and surface temperatures, the higher amounts were due to differences in simulated SSTs and not so much because of temperature advections. It should be emphasized that the latent heat flux showed no negative values, while the sensible heat flux was less than zero when the SST was colder than the air temperature in both simulations.

5 Conclusions

The physical problem of this study was the assessment of the importance of the correction of the SST for specification in the meteorological models in terms of the impact on the development and evolution of transient weather systems, obtaining certain important results in the simulations.

The importance of the correction of the SST through the OML within the BRAMS seemed to be pertinent since the transient systems may modify the surface flows in less than 1 day.

In terms of the use of computing resources, the activation of the OML module in the BRAMS module did not significantly affect the performance of the simulations (about 2 hours longer than the control case) and did not compromise the performance of the experiments, which are important when considering an operational routine.

In general, the SST anomalies did not present latitudinally distributed patterns, but rather isolated clusters of variations. The active OML initially modified the SST, and there was an increase in H and LE, and they subsequently reached medium to high levels, always associated with deeper events (lifting of air due to cyclones or fronts).

It was clear that the inclusion of the active OML in the BRAMS routine did not significantly affect the jets at high levels. The few differences in this variable were probably related to the different shifts in convective patterns. However, differences in the vorticity advection at 500 hPa indicated a change in the trajectory of the transients. These differences in the displacements of systems were discreetly observed through the pressures and variations (in direction and mainly in intensity) of the winds. In general, in light (intense) winds, the differences between the simulations decreased (increased), regardless of the atmospheric phenomenon in action.

The pressure drops were not significant (1 hPa), so that changes in the surface flow may be related to the maintenance/persistence of the systems, advancing or delaying their displacement rather than changes in their intensity.

However, it should always be emphasized that the K-T CMO model is thermodynamic and reacted well to its purpose. The considerable deepening and cooling observed in the HYCOM simulations are due to ocean circulation factors (advection by currents, mixing by the wind increasing the TKE, Ekman pumping, etc.). For such precision it would be necessary to direct the study to the coupling of atmospheric and ocean models, which is beyond the scope of this article.

Finally, the importance of this study focuses on the inclusion of a simplified OML model in the atmospheric model as a low-cost computational solution and, for short periods, it was shown to be efficient in the improvement of surface flows, which often make the difference in the transient atmospheric phenomena, as in the case of extratropical cyclones. However, the absence of large variations in the other variables in all simulations was probably due to the response time of the variation of the SST not being enough to cause major changes on the large atmospheric scale.

6 Acknowledgments

This work was funded by Coordenação de Aperfeiçoamento de Pessoal de Nível Superior (CAPES) and Conselho Nacional de Desenvolvimento Científico e Tecnológico (CNPq).

The authors would like to acknowledge Dr Edmilson Freitas, professor at IAG/USP for the contribution in BRAMS numerical modeling.

7 References

Bleck, R. 2002. An oceanic general circulation model framed in hybrid isopycnal-cartesian coordinates. *Ocean Modelling, 4*: 55–88.

Bosart, L.F. & Lackmann, G.M. 1995. Post-landfall tropical cyclone reintensification in a weakly-baroclinic environment: A case study of hurricane David (September 1979). *Monthly Weather Review, 123*: 3268-3291.

Carroll, M.L.; DiMiceli, C.M.; Sohlberg, R.A. & Townshend, J.R.G. 2003. 250m MODIS Normalized Difference Vegetation Index, *University of Maryland, College Park, Maryland*, Day 289. Available at: http://glcf.umd.edu/data/ndvi

Chen, C. & Cotton, W.R. 1983. A one-dimensional simulation of the stratocumulus-capped mixed layer. *Boundary-Layer Meteorology*, *25:* 289-321.

Chu, P.C. 1993. Generation of low frequency unstable modes in a coupled equatorial troposphere and ocean mixed layer. *Journal of the Atmospheric Sciences, 50:* 731-749.

Fazenda, A.L.; Demerval S.M.; Enari E.H.; Panett J. & Rodrigues L.F. 2006. *First Time User's Guide (BRAMS Version 3.2). CPTEC,* Ver.2, 4-5.

Freitas, S.R.; Panetta, J.; Longo, K.M.; Rodrigues, L.F.; Moreira, D.S.; Rosário, N.E.; Silva Dias, P.L.; Silva Dias, M.A.F.; Souza, E.P.; Freitas, E.D.; Longo, M.; Frassoni, A.; Fazenda, A.L.; Santos e Silva, C.M.; Pavani, C.A.B.; Eiras, D.; França, D.A.; Massaru, D.; Silva, F.B.; Santos, F.C.; Pereira, G.; Camponogara, G.; Ferrada, G.A.; Campos Velho, H.F.; Menezes, I.; Freire, J.L.; Alonso, M.F.; Gácita, M.S.; Zarzur, M.; Fonseca, R.M.; Lima, R.S.; Siqueira, R.A.; Braz, R.; Tomita, S.; Oliveira, V. & Martins, L.D. 2017. The Brazilian developments on the Regional Atmospheric Modeling System (BRAMS 5.2): an integrated environmental model tuned for tropical areas, *Geoscientific Model Development, 10:* 189-222.

Friehe, C.A.; Shaw, W.J.; Rogers, D.P.; Davidson, K.L.; Large, W.G.; Stage, S.A.; Crescenti, G.H.; Khalsa, S.J.S.; Greenhut, G.K. & Li, F. 1991. Air-sea fluxes and surface layer temperatures around a sea-surface temperature front. *Journal of Geophysical Research, 96:* 8593-8609.

Gan, M.A. & Rao, V.B. 1991. Surface Cyclogenesis over South

America. *Monthly Weather Review, 119:* 1293-1302.

Gevaerd, R. & Freitas, S.R. 2006. Estimativa operacional da umidade do solo para iniciação de modelos de previsão numérica da atmosfera. Parte I: Descrição da metodologia e validação, *Revista Brasileira de Meteorologia, 21(3):* 1-15.

Grell, G.A. & Devenyi, D. 2002. A generalized approach to parameterizing convection combining ensemble and data assimilation techniques. *Geophysical Research Letters, 29:* 1-4.

Hart, R.E. 2003. A cyclone phase space derived from thermal wind and thermal asymmetry. *Monthly Weather Review, 131:* 585-616.

IGBP. 1986. The International Geosphere–Biosphere Programme: A study of global change. *In:* ICSU 21st GENERAL ASSEMBLY, Berne, Switzerland, 1986. IGBP Report No. 1, ISSN 0284-8015: 21.

Kalnay, E.; Kanamitsu, M.; Kistler, R.; Collins, W.; Deaven, D.; Gandin, L.; Iredell, M.; Saha, S.; White, G.; Woollen, J.; Zhu, Y.; Leetmaa, A.; Reynolds, B.; Chelliah, M.; Ebisuzaki, W.; Higgins, W.; Janowiak, J.; Mo, K.C.; Ropelewski, C.; Wang, J.; Jenne, R. & Joseph, D. 1996. The NCEP/NCAR 40-year reanalysis project. *Bulletin of the American Meteorological Society, 77:* 437-471.

Kraus, E.B. & Turner, J.S. 1967. A one-dimensional model of the seasonal thermocline II, the general theory and its consequences. *Tellus, 19:* 98-105.

Levitus, S. & Boyer, T.P. 1994. *World Ocean Atlas 1994* Volume 4: Temperature. NOAA Atlas NESDIS 4

Mellor, G.L. & Yamada, T. 1982. Development of a turbulence closure-model for geophysical fluid problems. *Reviews of Geophysics, 20:* 851-875.

Necco, G.V. 1982. Comportamiento de vórtices ciclónicos en el área sudamericana durante el FGGE: Ciclogenesis. *Meteorológica, 8:* 7-20.

Palmeira, R.M.J. 2003. *Climatologia de ciclones extratropicais na região da América do Sul.* Departamento de Meteorologia, Universidade Federal do Rio de Janeiro, Monografia de Bacharelado em Meteorologia. 39p.

Pezzi, L.P.; Souza, R.B.; Dourado, M.S.; Mata, M.M.; Garcia, C.A.E. & Dias, M.A.F.A.S. 2005. Ocean-atmosphere in situ observations at the Brazil-Malvinas Confluence region. *Geophysical Research Letters, 32:* 1-4.

Reboita, M.S., 2008. *Ciclones Extratropicais sobre o Atlântico Sul: Simulação Climática e Experimentos de Sensibilidade*. Programa de Pós-Graduação em Meteorologia. Universidade de São Paulo, Tese de Doutorado, 294p.

Saraiva, J.M.B. 1996. *Previsão de tempo na região sul: efeitos locais e influência da liberação de calor latente*. Programa de Pós-Graduação em Meteorologia. Universidade de São Paulo, Tese de Doutorado, 201p.

Seluchi, M.E. 1995. Diagnóstico y pronóstico de situaciones sinópticas conducentes a ciclogénesis sobre el este de Sudamérica. *Geofísica Internacional, 34 (2):* 171-186.

Sinclair, M.R. 1995. A Climatology of Cyclogenesis for the Southern Hemisphere. *Monthly Weather Review, 123:* 1601-1619.

Silva Dias, M.A.F.; Rutledge, S.; Kabat, P.; Silva Dias, P.L.; Nobre, C.; Fisch, G.; Dolman, A.J.; Zipser, E.; Garstang, M.; Manzi, A.O.; Fuentes, J.D.; Rocha, H.R.; Marengo, J.; Plana-Fattori, A.; Sá, L.D.A.; Alvalá, R.C.S.; Andreae, M.O.; Artaxo, P.; Gielow, R. & Gatti, L. 2002. Clouds and rain processes in a biosphere atmosphere interaction context in the Amazon Region. *Journal of Geophysical Research: Atmospheres, 107:* 8072-8072.

Silva, R.R.; Silva Dias, P.L.; Gandu, A. & Moreira, D.S. 2004. Impactos da temperatura da superfície do mar no ciclone Catarina. *In:* CONGRESSO BRASILEIRO DE METEOROLOGIA, Rio de Janeiro, 2004. Anais do XIII Congresso Brasileiro de Meteorologia, Fortaleza, CE.

Smagorinsky, J. 1963. General circulation experiments with the primitive equations. I. The basic experiment. *Monthly Weather Review, 91:* 99-164.

Sugahara, S. 2000. Variação anual da frequência de ciclones no Atlântico Sul. *In:* CONGRESSO BRASILEIRO DE METEOROLOGIA, Rio de Janeiro, 2000. Anais do XI Congresso Brasileiro de Meteorologia, Rio de Janeiro, RJ, p. 2607-2612.